Available online at www.sciencedirect.com

ScienceDirect

Energy Procedia 00 (2014) 000–000

Energy Procedia

www.elsevier.com/locate/procedia

GHGT-12

CO_2-DISSOLVED: a Novel Concept Coupling Geological Storage of Dissolved CO_2 and Geothermal Heat Recovery – Part 4: Preliminary Thermo-Hydrodynamic Simulations to Assess the CO_2 Storage Efficiency

V. Hamm[a], C. Kervévan[a,]*, D. Thiéry[a]

[a] *BRGM, 3 av. Claude Guillemin, BP 36009, 45060 Orléans Cedex 2, France*

Abstract

The CO_2-DISSOLVED project aims at assessing the technical-economic feasibility of coupling CO_2 storage in a saline aquifer and geothermal heat recovery. The proposed infrastructure basically relies on a standard geothermal doublet where CO_2 would be injected after having been entirely dissolved in the cooled brine. The objective of this preliminary thermo-hydrodynamic modeling study was to quantify the expected CO_2 storage lifetime and efficiency. The results first confirmed that CO_2 will inevitably be produced in the extracted brine after 2-15 years of continuous injection, depending on the operating parameters. However, mass balance calculations evidenced that after a 30 year injection period, 37-85% of the total CO_2 injected should remain stored in the aquifer.
© 2013 The Authors. Published by Elsevier Ltd.
Selection and peer-review under responsibility of GHGT.

Keywords: CO_2 storage; dissolved CO_2; geothermal energy; saline aquifer; thermo-hydrodynamic modeling; storage efficiency

1. Introduction

This study was conducted in the framework of the CO_2-DISSOLVED project [1], funded by the ANR (French National Research Agency). This project proposes to assess the feasibility of a novel CO_2 injection strategy in deep

* Corresponding author. Tel.: +33-2-38-64-25-09; fax: +33-2-38-64-33-34.
E-mail address: c.kervevan@brgm.fr

1876-6102 © 2013 The Authors. Published by Elsevier Ltd.
Selection and peer-review under responsibility of GHGT.

saline aquifers, combining injection of dissolved CO_2 (instead of supercritical CO_2) and recovery of the geothermal heat from the extracted brine. This approach relies on the closed-loop geothermal doublet technology where the warm water is extracted at the production well and the cooled brine is re-injected in the same aquifer via a second well (injection well).

The objective of the work presented here was to provide first quantitative elements to assess the feasibility of the concept in terms of storage lifetime and efficiency. For that purpose, we performed hydrodynamic modeling of several test-cases relying either on the conventional doublet technology (deviated injection and production wells), or on a set of three wells (one injector / two producers, or conversely). A third case was also investigated using a horizontal well architecture instead of a typical deviated well for the injection. The selected hydrodynamic parameters are typical of the deep geothermal resources of the Paris basin (Dogger aquifer). Several distances between wells and production flow rates were simulated. In those preliminary simulations, the dissolved CO_2 was considered as a non-reactive tracer with no impact on the CO_2 laden brine properties (viscosity and density), and no chemical reactivity. We also performed some simulations accounting for coupling with heat transfer (dependency of brine viscosity and density upon temperature).

The first part of this paper describes the conceptual model on which our simulations were based on. The second part of the paper deals with the results achieved for the various scenarios simulated. The results presented focus more specifically on both the general hydrodynamic behavior of the system, and the storage efficiency defined here as a mass balance ratio between the CO_2 actually stored in the aquifer and the total CO_2 injected at the end of the injection period.

2. Modeling approach

Nomenclature

Variables

C	concentration of dissolved CO_2 in the aquifer ($M.L^{-3}$)
d	distance between the wells of the doublet, bottom hole (L)
dm/dt	accumulation term in the dissolved CO_2 mass balance equation ($M.T^{-1}$)
dr/dt	source/sink term in the dissolved CO_2 mass balance equation ($M.T^{-1}$)
m	mass of dissolved CO_2 in the aquifer (M)
P	pressure ($M.L^{-1}.T^{-2}$)
Q	CO_2 laden brine volumetric flow rate of injection ($L^3.T^{-1}$)
S	salinity ($M.L^{-3}$)
T	temperature (K)
τ	injection period (T)
R	thermal retardation factor (-)
V_e	effective pore velocity ($L.T^{-1}$)
V_{th}	thermal front velocity ($L.T^{-1}$)
ω	porosity (-)
$\rho_A C_A$	Aquifer global heat capacity ($J.L^{-3}.K^{-1}$)
$\rho_F C_F$	fluid heat capacity ($J.L^{-3}.K^{-1}$)

Superscripts

$\dot{}$	rate of the corresponding variable, with respect to time (e.g. mass rate)

Subscripts

inj	at the injection well
prod	at the production well
stored	stored in the aquifer

2.1. Conceptual hydrodynamic model

The conceptual model relies on a 2D single-layer geometry for the flow and CO_2 non-reactive tracer transport calculations, and on a pseudo 3D multilayer model for the coupled flow, CO_2 and heat transport calculations. The finite volume code MARTHE, developed at BRGM [2, 3], has been used for the simulations. The reservoir model is based on homogeneous hydraulic and thermal properties. The horizontal dimensions of the domain are 20 x 10 km divided in rectangular cells of 100 x 100 m, with a horizontal refinement of 20 x 20 m in the vicinity of the wells (Fig. 1). The layer thickness is 20 m, which is representative of the cumulated average thickness of the productive layers in the Dogger aquifer. In the case of heat transport calculation with dependency of fluid viscosity and density upon temperature, the aquifer layer is refined and both base and cap-rock layers were added. Heat conduction in base and cap-rock is solved in z direction using a semi-analytical solution developed by Vinsome and Westerfeld [4] added to 3D numerical heat calculation (conduction plus advection) in the aquifer layers.

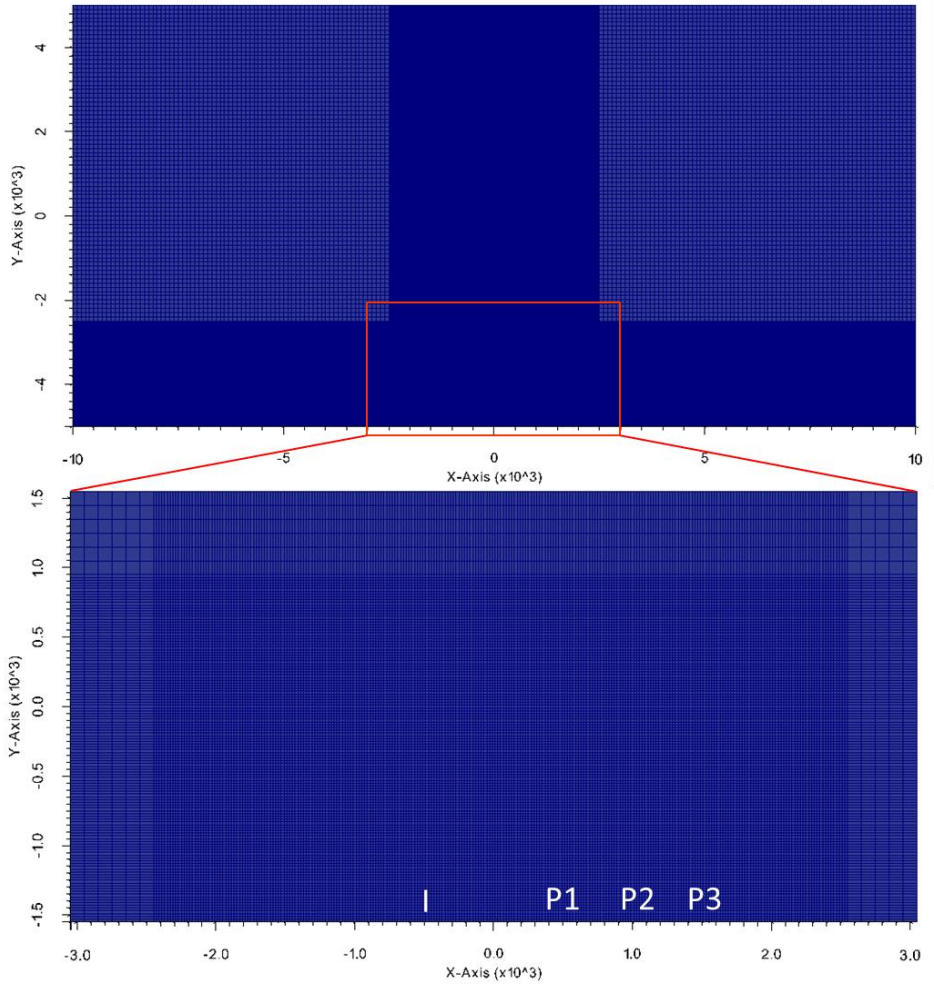


Fig 1. Top view of the meshing and different wells locations (I: injection well, P: production well at different distance from the injector (P1: 1 km, P2, 1.5 km or P3: 2 km

The parameters used for the thermo-hydrodynamic simulations are summarized table 1. They are typical measurements as flow meter log, well testing, plug measurements representative of the Dogger aquifer.

Table 1: Model parameters

Parameters	Values
Rock porosity	0.15 [-]
Specific storativity	10^{-6} [m^{-1}]
Average aquifer transmissivity	40 [Dm]
Average aquifer temperature	70 [°C]
Fluid density	0.4 [mPa.s]
Average fluid salinity	20 [g/l]
Fluid heat conductivity	0.6 [W/m/°C]
Fluid heat capacity	4.18 [MJ/m^3/°C]
Rock heat conductivity	2.5 [W/m/°C]
Rock heat capacity	2.2 [MJ/m^3/°C]
Longitudinal heat diffusivity	20 [m]
Transversal heat diffusivity	10 [m]

2.2. CO_2 mass balance calculation

In order to quantify the amount of CO_2 effectively stored in the aquifer at the end of a simulated injection period, we first applied a general mass balance equation according to which:

$$\overline{m_{inj}} + \frac{dr}{dt} = \overline{m_{prod}} + \frac{dm}{dt} \tag{1}$$

Introducing more familiar variables such as concentration (C) and volumetric flow rate (Q), equation (1) can be rewritten as:

$$Q.C_{inj} + \frac{dr}{dt} = Q.C_{prod} + \frac{dm}{dt} \tag{2}$$

In these simulations, we considered that no chemical reaction occurred. As a consequence, it can be reasonably assumed that the source/sink term in the above equations can be omitted ($dr/dt = 0$). Hypothesizing a constant flow rate all along the injection period (τ), we can then easily infer from equation (2) the total mass of CO_2 accumulated in the aquifer (m_{stored}):

$$m_{stored} = \int_0^\tau \frac{dm}{dt} dt = Q \int_0^\tau \left(C_{inj} - C_{prod}\right) dt \tag{3}$$

C_{inj} is considered as a constant term in our simulations, and C_{prod} is an output of the hydrodynamic model that is tabulated at every time step, so that the integral can be easily calculated using classical integration algorithms included in general purpose numerical computation software (we used a short Scilab script to calculate the integral in equation (3)).

3. Results and discussion

All the simulations presented here assumed no chemical interaction between the brine and the porous matrix of the aquifer. Similarly, dissolved CO_2 was assumed to behave as a non-reactive tracer; in particular, the effect on

brine density and brine viscosity were not accounted for. Only the temperature effect on water properties (viscosity, density) was accounted for in the simulations considering heat transfer.

Consequently, in all the calculations, the CO_2 concentration in the injected water was assumed to be constant all along the injection period; the absolute value of this concentration was then meaningless, that is why most of the results involve a dimensionless relative concentration comprised between 0 and 1 (ratio of the CO_2 concentration in water to the CO_2 concentration in the injected water). For the mass balance calculations however, we assumed a CO_2 concentration in the injection water of 50 $g.L^{-1}$ (approximately 1 $mol.L^{-1}$) which is a reasonable order of magnitude for CO_2 solubility in the typical (*P, T, S*) conditions of the exploited geothermal aquifers of the Paris basin (e.g., see fig. 4 in [5]).

3.1. Single doublet, without heat transfer

This first series of simulations aimed at quantifying the effect of the key operating parameters of the doublet system, *i.e.* the distance between the well shoes, and the injection flow rate. Three typical distances between wells (1, 1.5, and 2 km) and flow rates (100, 200, and 300 $m^3.h^{-1}$) were investigated, all being typical of actual operating parameters of the geothermal doublets of the Paris basin. One of the primary questions to answer was about the quantification of the CO_2 migration time in the aquifer between the injection and the production wells. In a doublet system, the fact that an injected product is going to be present in the extracted brine after a while (at increasing concentration with time in case of continuous injection), is inevitable. In our simulations where injection is continuous, CO_2 is considered as a tracer. Consequently, it is expected to be present at the production well after a certain period to be determined by our calculations.

The results provide quantitative estimates of the concentration of the CO_2 produced at the extraction well and on the timeframe of the mass transport process.

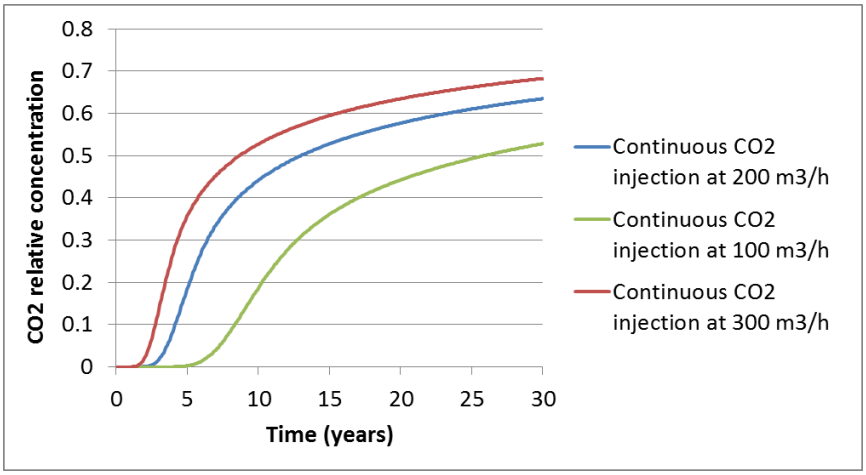


Fig. 2. CO_2 breakthrough at the production well for continuous injection at various flow rates. The injection and production well shoes are located 1.5 km apart (P2 in Fig 1).

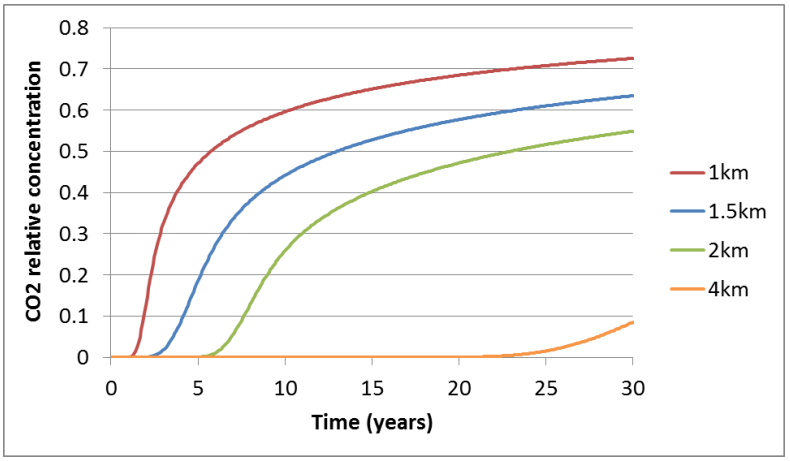


Fig. 3. CO_2 breakthrough at the production well for continuous injection with various distances between the injection and the production well shoes (P1, P2 or P3). The injection flow rate is constant at 200 $m^3.h^{-1}$.

Unsurprisingly, the curves on Fig. 2 clearly show, at a given distance between wells (1.5 km in this case), that the higher the flow rate, the shorter the CO_2 breakthrough time at the production well, and the higher the CO_2 concentration in the extracted brine. It takes approximately 2 to 8 years in this example to get a 0.1 relative concentration. On Fig. 3, the effect of the distance between wells is evidenced: the higher it is, the higher the breakthrough time is and the lower the CO_2 concentration is. For a distance of 4 km between the wells, the threshold concentration value of 0.1 is not reached at the end of a 30 year continuous injection period.

Consequently, for an efficient CO_2 storage using a doublet system, it seems at first glance that we should have to minimize the flow rate and maximize the distance between wells. However, simple technical reasons prevent us from choosing the distance between wells we would like to have: for instance, in the geothermal reservoirs of the Paris basin, the depth of the productive layers of the Dogger aquifer is, on average, between 1,500 and 2,000 m. With the constraint of a typical distance between the well heads of a few meters (for minimal surface footprint and heat loss), and a limit of 55° in the deviation angle, the maximum distance between the well shoes cannot exceed 1.5 to 2 km. So, the distance of 4 km between wells presented on Fig. 3 is actually an ideal case but such a doublet could not be implemented in the context of the currently exploited geothermal aquifer of the Paris basin. On the other hand, decreasing the flow rate would decrease the CO_2 mass injected as well as the quantity of geothermal energy recoverable.

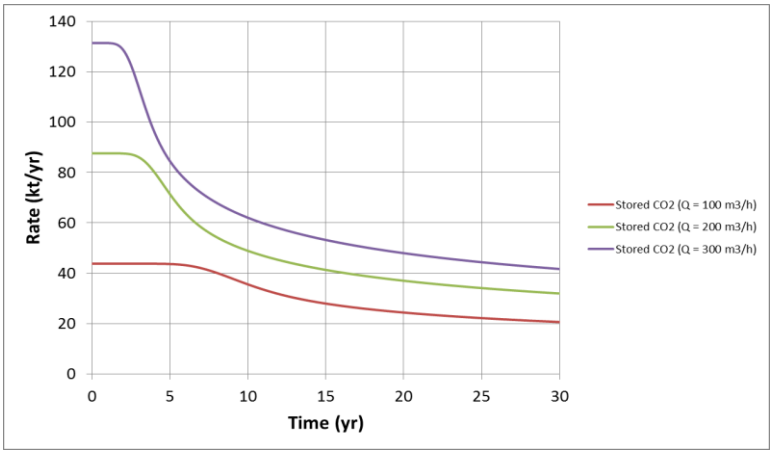


Fig. 4. Evolution of the stored CO_2 rate all along a 30 year injection period, as a function of the injection flow rate (Q). The injection and production well shoes are located 1.5 km apart.

However, the most important point to consider when studying a system basically dedicated to CO_2 storage is to determine how much CO_2 will be effectively stored at the end of an injection period. Based on the breakthrough curves presented previously, it is demonstrated that CO_2 is going to be produced at the extraction well after a few years of injection. Even though this produced CO_2 is not going to be released to the atmosphere because the injection-production wells work in closed-loop, these results strongly suggests that part of the injected CO_2 is not going to remain stored in the aquifer. In terms of mass balance however, equation (3) demonstrates that since C_{prod} remains lower than C_{inj} *(i.e.* relative concentration remains strictly lower than 1), the mass of CO_2 stored is then necessarily greater than 0; so, CO_2 storage is going to be effective.

In order to quantify more precisely the amount of stored CO_2, we first reworked the data of Fig. 2 to express them in terms of storage rate (Fig. 4). The results confirm the general trend observed on Fig. 2 according to which the lower flow rate provides a less and later significant decrease in the storage rate. However, it is important to remark that, even though a very significant decrease in the storage rate is observed relatively early (after 2-3 years of injection) for the highest flow rate of injection (300 $m^3.h^{-1}$), this storage rate always remains greater than for the lower flow rates.

Now, performing a numerical integration of equation (3) for all the operating parameters, we were able to calculate the cumulated masses of stored CO_2 over the 30 year injection period considered in these simulations. The results are synthesized on Fig. 5. They clearly illustrate the impact of both the distance and the flow rate on the accumulated mass of CO_2 effectively stored in the aquifer: for a given flow rate, the accumulated mass increases with the distance; for a given distance, the stored mass increases with the flow rate.

For a better interpretation of these results, it is interesting here to introduce the notion of storage efficiency that we define, for a given injection period, as the percentage of the mass of CO_2 effectively stored in the aquifer with respect to the mass injected. On Fig. 6, the results expressed in terms of storage efficiency provide a new insight on the understanding of the storage system: to maximize the efficiency of the storage, it is necessary to work with the lowest flow rate (100 $m^3.h^{-1}$) and the highest distance between the wells shoes (2 km); however, with these parameters, the absolute value of the total mass of CO_2 stored after 30 years (1,118 kt) is surprisingly lower than for the least efficient case (Q = 300 $m^3.h^{-1}$; d = 1 km) where the mass of CO_2 stored reaches 1,447 kt.

At this stage however, it is too early to draw definitive conclusions on the best strategy to select: optimizing the storage efficiency or maximizing the total amount of stored CO_2. Other aspects have to be considered first: optimization of the geothermal energy recovered as a function of the needs, expected lifetime of the doublet, configuration of the site (surface and subsurface), economic aspects, etc. This will be treated later in the project, when application test cases will have been selected.

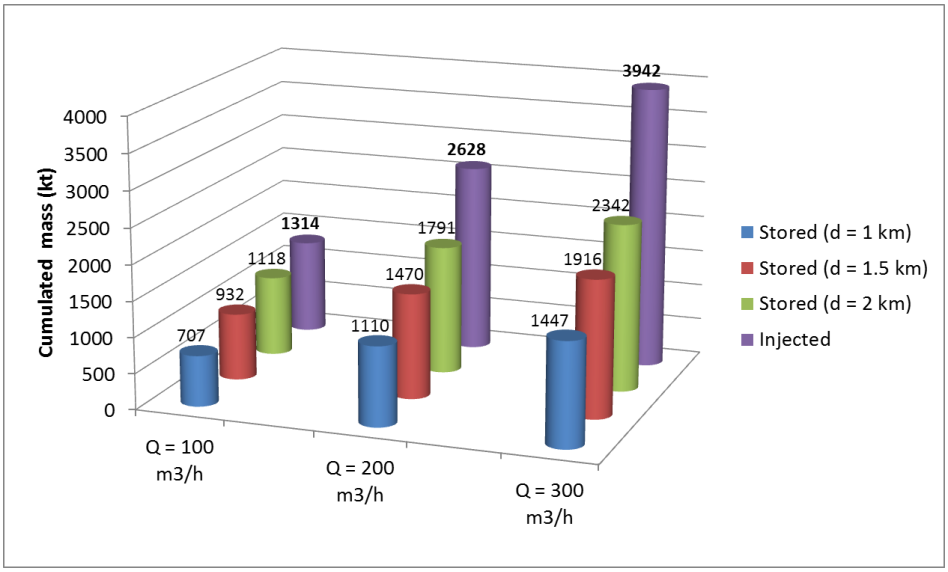


Fig. 5. Comparison between the cumulated masses (in kt) of stored and injected CO_2 over a period of 30 years of continuous injection, as a function of the distance between wells (*d*) and the injection flow rate (*Q*).

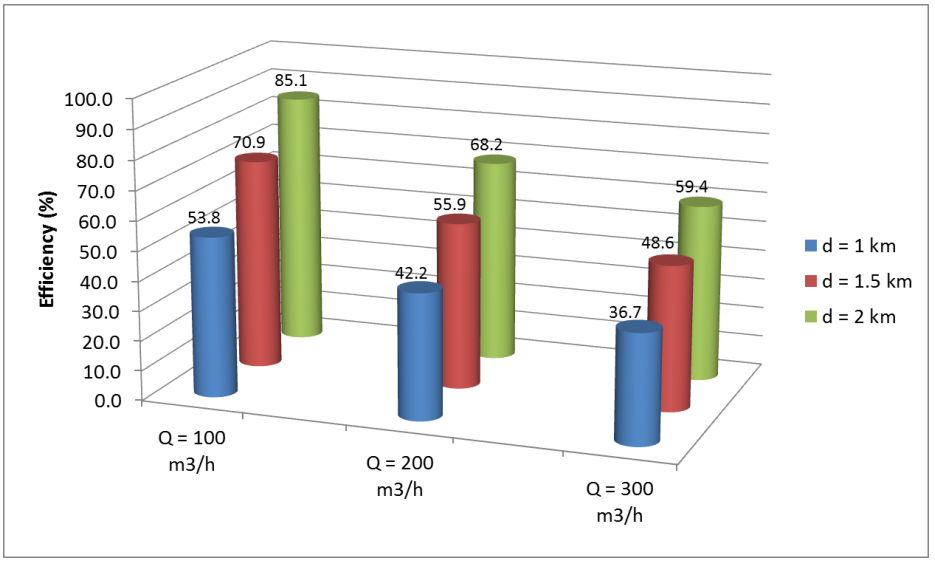


Fig. 6. Storage efficiency over a period of 30 years of continuous injection, as a function of the distance between wells (*d*) and the injection flow rate (*Q*).

3.2. Single doublet with heat transfer

In this second set of simulations, we simulated the coupling of heat transport and non-reactive tracer CO_2 mass transport by taking into account brine density and viscosity dependence on temperature (thermal coupling). The conditions used for these simulations are a constant flow rate of 200 $m^3.h^{-1}$, a distance between wells of 1,500 m and a re-injected fluid temperature of 40 °C. The initial fluid temperature was set to 70°C which is the average temperature of the Dogger aquifer in the Paris basin.

Figure 7 shows the concentration of the CO_2 produced at the extraction well on the left axis versus the production temperature on the right axis. There is a retardation factor of about 4 between the thermal breakthrough and the tracer breakthrough. This retardation factor can be expressed by equation (4):

$$R = \frac{V_e}{V_{th}} = \frac{\rho_A C_A}{\omega \rho_F C_F} \tag{4}$$

Consequently, after 30 years of geothermal exploitation, the production temperature drop is less than 0.5°C, which is not significant compared to the relative CO_2 concentration variation at the same date. Furthermore, the comparison between the growth of the CO_2 plume and of the thermal plume show a great difference of the domain impacted (Fig. 8). This process is due to the important role of the base and cap rock that slow down the propagation of the thermal front. The effect of temperature on brine properties and consequently on the tracer velocity is limited and results only in a slightly higher breakthrough time and lower relative concentrations at the production well. Indeed, as the doublet flow rate is maintained constant (prescribed flow rate), an increase in fluid viscosity around the injector due to the cooling implies a slight increase in pressure gradient between wells with constant velocity. The effect of temperature upon density (at constant salinity) is negligible for the thickness considered. In a later stage, the effect of dissolved CO_2 on fluid viscosity and density should be considered.

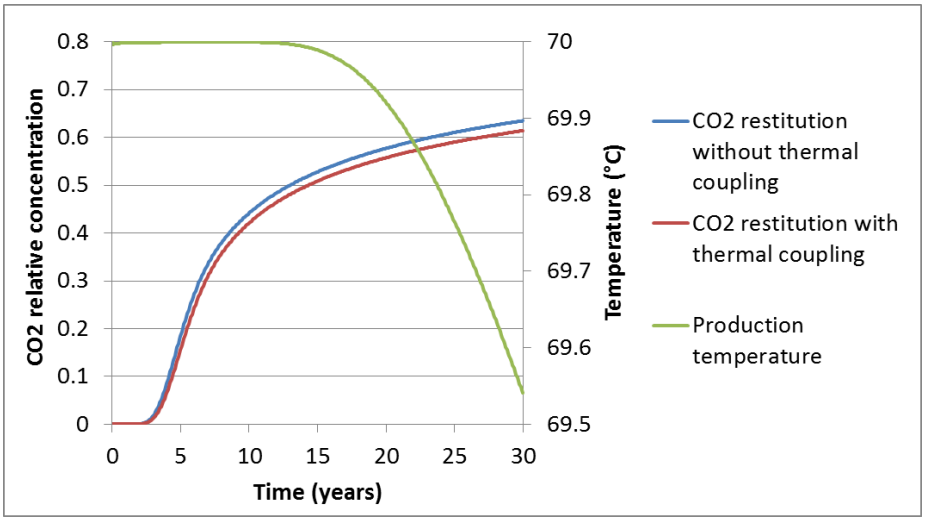


Fig 7. CO2 and thermal breakthrough at the production well for continuous injection

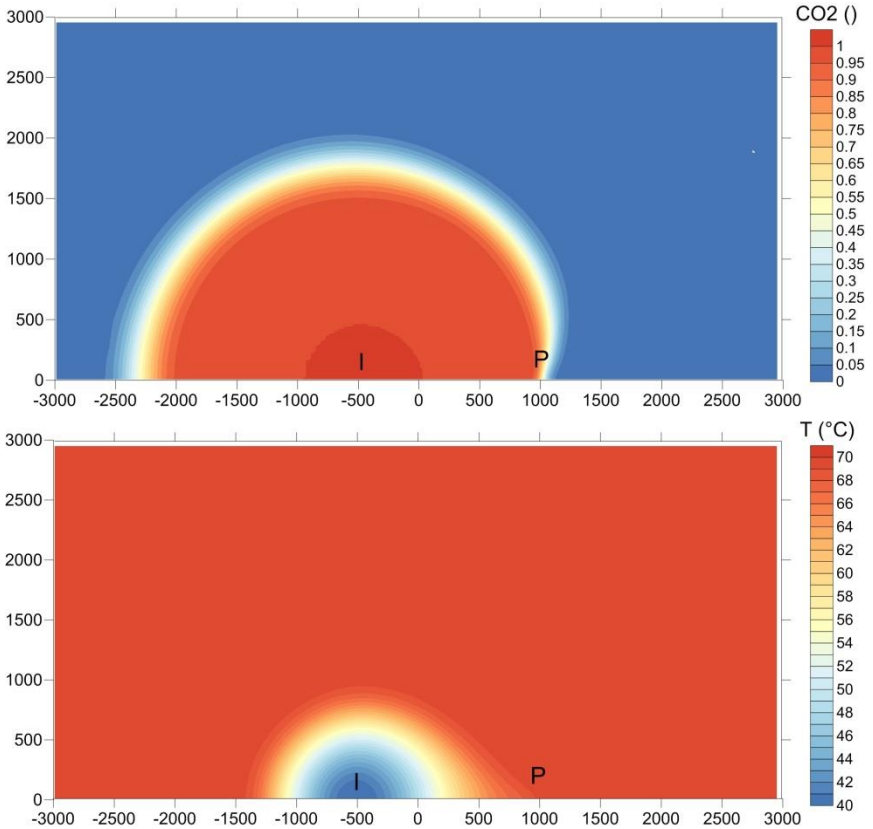


Fig 8. Size of CO2 and thermal plumes after 30 years of continuous injection

Fig. 9 and 10, based on the same principle as in §3.1, show respectively the evolution of the stored CO_2 rate with time, and the total mass of CO_2 stored and the storage efficiency after a period of 30 years for both cases (with and without thermal coupling). These figures confirm that the change in temperature does not change much the stored

CO_2 rate and, as a consequence, the total mass stored after 30 years of injection of a cold CO_2-rich solution. In these examples, it then appears that the temperature of the injected fluid has less influence for the CO_2 storage than for the geothermal heat exploitation.

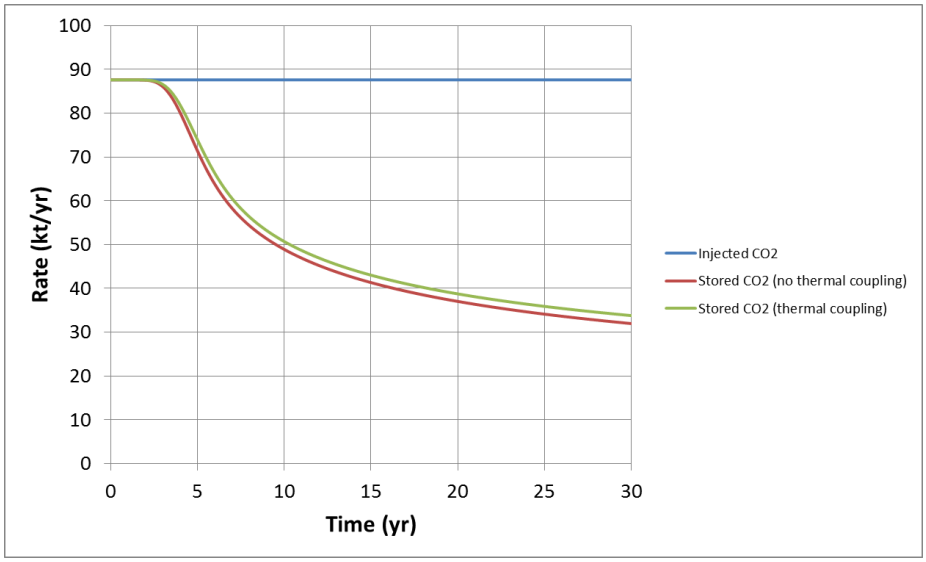


Fig. 9. Evolution of the stored CO_2 rate all along a 30 year injection period

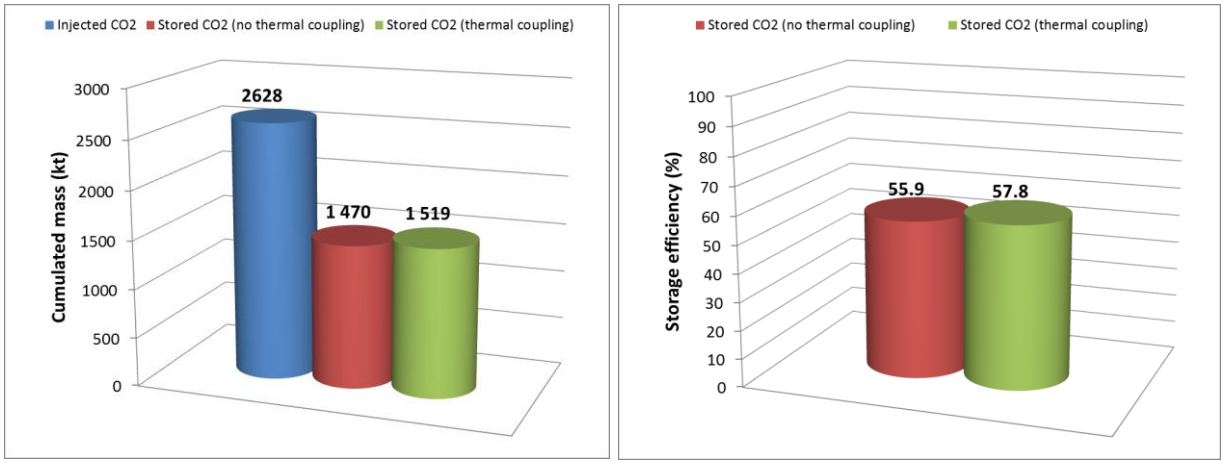


Fig. 10. Comparison between the cumulated masses (in kt) and the storage efficiency of stored CO_2 over a period of 30 years of continuous injection

3.3. Other wells configurations

In this last section, with an objective of improving the storage efficiency, we tested some other wells configurations such as a set of three wells (triplet) instead of a doublet or the use of a horizontal or sub-horizontal well for injection. The horizontal well technology is already used in oil or gas industry extraction and a first case is envisaged for both production and injection in the Dogger aquifer for geothermal purpose. In the next figures, the

notation used are ‘IP’ for a classical doublet with one injection and one production well, ‘PIP’ or ‘IPI’ in the case of an alignment of three wells with one central injector and two producers, or two injectors surrounding a central producer, respectively. The ‘IIP’ configuration, with one producer and two injectors grouped together was also tested hereafter. The conditions for the simulations are identical to the §3.1 case, *i.e.* no thermal effect, a constant total flow rate of 200 $m^3.h^{-1}$ (divided evenly between the two injectors or producers), and a distance between each wells of 1,500 m. This distance is maximised with respect to the wells configuration (one central vertical well and two deviated wells). Nevertheless, the drilling of recent new wells in the Dogger aquifer is currently using two deviation angles at different depths leading to an increase in the distance between well shoes. In the case of a horizontal drain for the injection, the length is considered to be 1,000 m.

Figure 11 compares the CO_2 relative concentration at the production well for a classical doublet, three wells configurations, and 2 wells with one horizontal injection well. In the PIP or IPI cases, the CO_2 breakthrough time is delayed compared to the case of a doublet, but the concentration that reaches the production well(s) becomes higher than the one observed for a doublet after 10 years of production. In the IIP case, the CO_2 breakthrough time is also greater than for a doublet but the CO_2 relative concentration at the production well remains always significantly smaller than the one calculated for a doublet. Finally, in the case of a horizontal injection well, the CO_2 breakthrough time is the most delayed, but after 30 years of production, the CO_2 relative concentration remains smaller than for a classical doublet, but higher than for the IIP scheme.

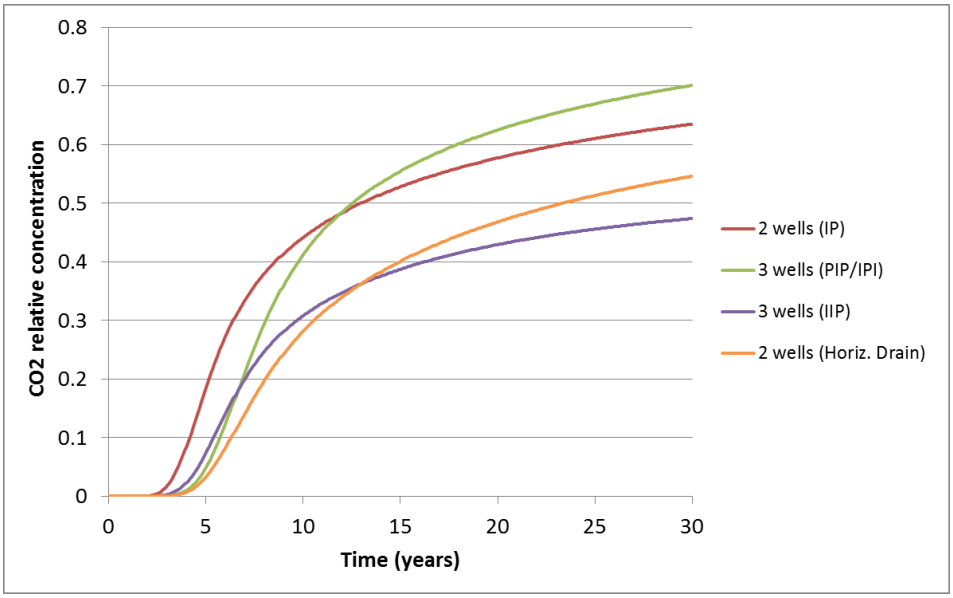


Fig. 11. CO_2 breakthrough at the production well for continuous injection and different wells configurations

Fig. 12 to 14 show the corresponding stored CO_2 rates and the total stored CO_2 and storage efficiency over an injection period of 30 years. They indicate that the IPI or PIP schemes does not improve the CO_2 storage efficiency and even slightly degrade it. In contrast, both the IIP and the horizontal injector schemes significantly improve the CO_2 storage efficiency (respectively 68.4% or 67.1% instead of 55.9% for a classical doublet).

Nevertheless, we have to keep in mind that we can also reach those rates with a classical doublet by decreasing the flow rate and/or increasing the wells distance (fig. 6). The benefit of those technical solutions using three wells or horizontal wells must also be balanced with their higher initial capital cost and the actual energy needs, in order to define an optimal injection scenario.

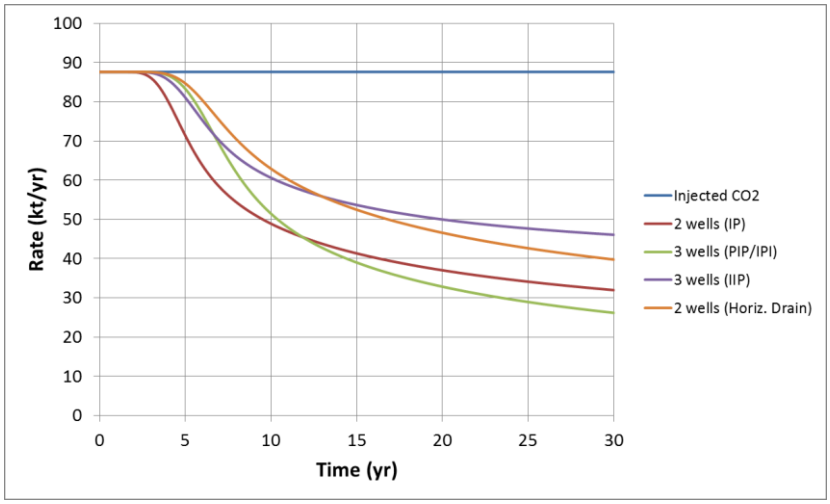


Fig. 12. Stored CO_2 rate for different wells configurations

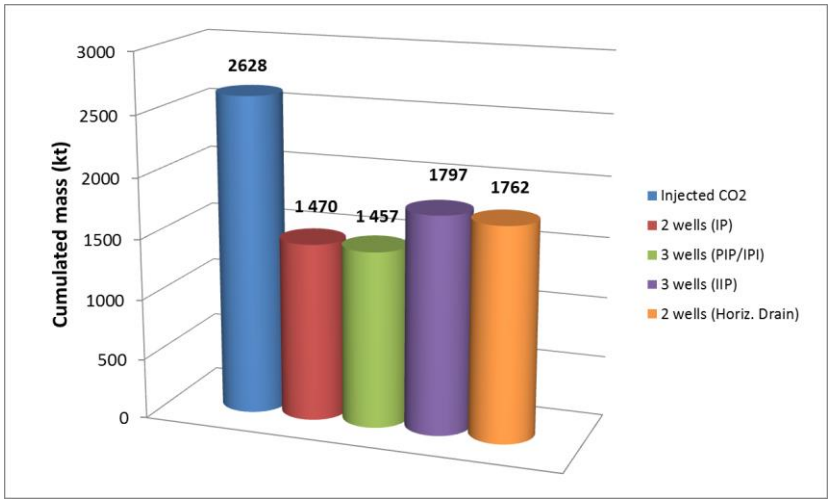


Fig. 13.Total Stored CO_2 mass for different wells configurations

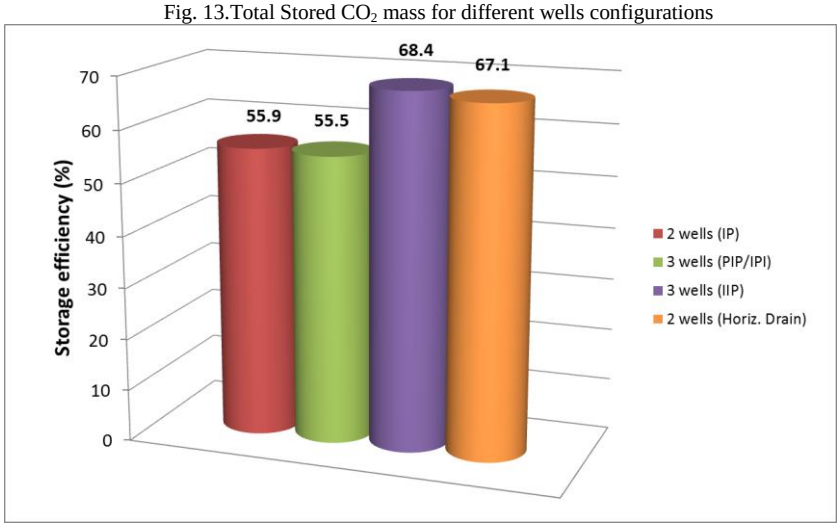


Fig. 14. Stored CO_2 efficiency for different wells configurations

4. Conclusion

This series of preliminary thermal-hydrodynamic simulations provides a first overview of the influence of the operating parameters and the wells configuration on the potential lifetime and efficiency of the CO_2 storage system. The results acquired so far demonstrate that:

- Dissolved CO_2 inevitably reaches the production well after a while. Typical breakthrough times obtained here range between 2 and 15 years for a technically achievable doublet in the context of the Dogger aquifer of the Paris basin. However, it has to be noticed that this CO_2 will not be released to the atmosphere since the production/heat exchanger/injection circuit is a closed loop. Increase in CO_2 concentration in the produced brine will then result in a lower quantity of gaseous CO_2 that could be dissolved at the injection well.

- The storage efficiency, defined here as the mass ratio between stored and injected CO_2, decreases with the flow rate, while it increases with the distance between the wells.

- For all the injection scenarios considered in our simulations, even the less favorable, a significant ratio of the injected mass of CO_2, varying from 37% to 85%, remains stored in the aquifer at the end of an injection period of 30 years (typical duration of an operating permit for a geothermal doublet in the Paris basin).

- Using a combination of two injection wells and one production well (triplet) or two wells with one horizontal injection well instead of a classical doublet, improves the storage efficiency (all equivalent operational parameters being equal). However, the required infrastructure would then be obviously more expensive; economic calculations applied to a well-defined test-case are necessary to conclude on the viability of those options.

In the next tasks of the project, more accurate simulations will be performed, accounting for both the effect of dissolved CO_2 on fluid viscosity and density, and the water/rock interaction processes. The combined effects of those chemical-physical processes is expected to slow down the migration velocity of dissolved CO_2 toward the production well of the doublet (or triplet). If this behavior is confirmed by numerical modeling, better storage efficiency will then be obtained, corroborating the conclusions of this study on the viability of the CO_2-DISSOLVED concept for achieving dissolved CO_2 storage in a saline aquifer exploited by a geothermal doublet (or triplet).

Acknowledgements

We would like to thank both the ANR (French National Research Agency) and the Research Directorate of BRGM for funding this study in the framework of the CO_2-DISSOLVED project. We are also grateful to the project team members for allowing us to publish these results.

References

[1] Kervévan C., Bugarel F., Galiègue X., Le Gallo Y., May F., O'Neil K., Sterpenich J. CO_2-DISSOLVED: a novel approach to combining CCS and geothermal heat recovery. In: EAGE, editor. Sustainable Earth Sciences, technologies for sustainable use of the deep sub-surface. Pau, France; 30 Sept.- 4 Oct. 2013.

[2] Thiéry D. Groundwater Flow Modeling in Porous Media Using MARTHE. in "Modeling Software Volume 5, Chapter 4, pp. 45-60 • Environmental Hydraulics Series". ISBN: 978-1-84821-157-5. Tanguy J.M., editor; Éditions Wiley/ISTE London. 2010.

[3] Thiéry D. Presentation of the MARTHE 7.4 code developed by BRGM. BRGM technical note NT EAU 2012/03 revised. 21 p. 2014.

[4]Vinsome P.K.W. and Westerfeld J.. A simple method for predicting cap and base rock heat losses in thermal reservoir simulators. JCPT 80-03-04.

[5] Kervévan C., Azaroual M., Durst P. Improvement of the Calculation Accuracy of Acid Gas Solubility in Deep Reservoir Brines: Application to the Geological Storage of CO_2. Oil Gas Sci. Technol., 60(2), pp. 357-379, 2005.